ORIGINAL RESEARCH PAPER
Volume - 15 | Issue - 02 | February - 2026 | PRINT ISSN No. 2277 - 8179 | DOI : 10.36106/ijsr
INTERNATIONAL JOURNAL OF SCIENTIFIC RESEARCH

COMPARATIVE OPTICAL ANALYSIS OF TRANSITION-METAL DISELENIDE (MSE_2) SINGLE CRYSTALS

Physics

R. D. Vaidya Seth P. T. Arts & Science College, Godhara
Kaushik R. Patel Microbiology Department, Gujarat Vidyapith, Ahmedabad

ABSTRACT

Single crystals of MSe_2 (M = Nb, Mo, Ta and W) were grown by chemical vapor transport technique using iodine as the transport agent. Optical absorption studies were performed on MSe_2 single crystals at room temperature in the vicinity of the fundamental absorption edge. Absorption spectra were recorded in the wavelength range 700–1400 nm using a UV–Vis–NIR DK-2A spectrophotometer. The experimental data were analyzed within the framework of a three-dimensional band structure model. This analysis revealed the involvement of both direct and indirect electronic transitions in the absorption process. Indirect transitions were found to be phonon-assisted and allowed, involving two phonons. The direct and indirect band gap energies, along with the associated phonon energies, were estimated for all investigated crystals. The obtained results are discussed in detail with respect to the electronic band structure and optical response of the transition metal diselenides.

KEYWORDS

INTRODUCTION

Transition metal dichalcogenides (TMDCs) have attracted considerable attention owing to their layered crystal structures and unique electronic and optical properties, which make them promising candidates for next-generation optoelectronic and photonic devices. Among these materials, transition metal diselenides (MSe_2, where M = Nb, Mo, Ta, and W) exhibit strong light–matter interactions, sizable band gaps in the visible–near-infrared region, and pronounced excitonic effects arising from reduced dimensionality and strong Coulomb interactions. These characteristics enable their application in photodetectors, solar cells, light-emitting devices, and nonlinear optical components [1–3].

Previous studies have reported that MSe_2 compounds can exhibit both direct and indirect electronic transitions, depending on the crystal thickness and electronic structure, with optical band gaps typically lying in the range of 1.3–1.6 eV [4,5]. Optical absorption and spectroscopic ellipsometry measurements have revealed high refractive indices, anisotropic dielectric responses, and critical -point transitions associated with interband electronic excitations [6]. Furthermore, first-principles calculations based on density functional theory have provided valuable insights into the electronic band structure, optical constants, and transition mechanisms of these materials, offering strong agreement with experimental observations [7,8].

Despite extensive investigations of thin films and monolayers, systematic experimental studies on the optical absorption behavior of bulk MSe_2 single crystals, particularly near the fundamental absorption edge, remain comparatively limited. In this context, the present work focuses on the growth of high-quality $NbSe_2$, $MoSe_2$, $TaSe_2$, and WSe_2 single crystals, and the investigation of their optical absorption properties at room temperature. Special emphasis is placed on identifying direct and indirect optical transitions, estimating the corresponding band gap energies, and analyzing phonon-assisted absorption processes using a three-dimensional band model.

Experimental

Layered single crystals of transition metal dichalcogenides MX_2 (M = IV_b V_b transition metal, X = S, Se, and Te) were grown by the chemical vapor transport (CVT) technique using iodine as a transporting agent. The stoichiometry of the as-grown crystals was confirmed using energy-dispersive X-ray analysis (EDAX). X-ray diffraction (XRD) analysis was performed for the structural characterization of the as-grown crystals. X-ray diffractograms were obtained using a Philips X-ray diffractometer (model: PW1820) with CuK radiation. All samples were grown using the chemical vapor transport technique. The as-grown samples exhibited p-type conductivity with a hole concentration of 10^{13} to 10^{16} cm^{-3} at room temperature.

Thin samples for absorption measurements were obtained by cleavage. The a and b axes are contained in the cleavage plane. Optical absorption data were obtained using a UV-VIS-NIR Spectrophotometer (Perkin Elmer, Model: Lambda –19). Prior to the measurement, the samples were oriented both optically and by back-reflection Laue techniques. Measurements were performed at room temperature with the electric field of the incident light parallel to the a and b crystallographic axes. Measurements along with the c-axis were not performed, because the crystal structure did not permit cutting and polishing. The energy range of the incident photons was extended from 1.0 to 1.5 eV.

Band Tailing

While impurity-band formation is an obvious consequence of increased impurity concentration, another important effect is the perturbation of the bands by the formation of tails of states, extending the bands into the energy gap. The problem of band tailing has received considerable theoretical attention [9-13]. An ionized donor exerts an attractive force on the conduction electrons and a repulsive force on the valence holes. Because impurities are distributed randomly in the host crystal, the local interaction will be strong, depending on the local crowding of the impurities. Dislocations are also usually present in the crystals. They occur at the edge of an extra plane of atoms. The misfit of such an extra plane results in compressional and dilutional strains, with the consequent onset of both lowering and raising the potential of the dislocation. Hence, one can say that impurities induce tails in the density states by perturbing the band edge via the deformation potential, Coulomb interaction, and forming a band of impurity states. The momentum-conserving transition between parabolic bands should result in an absorption edge that obeys the equation rgEhvAhv)(–=α, where r = ½, that is, where the absorption constant increases with the square root of the photon energy more than the gap energy. For a direct transition, one expects no absorption below the energy gap and, therefore, a steeply rising absorption edge. However, in practice, one usually finds an exponentially increasing absorption edge [14-16]. In several materials, d(lnα)/d (h) = 1/kT, which is known as Urbach's rule [17]. In the case of a degenerate p-type material, the Fermi level is taken to be in the parabolic portion of the valence band, so that the perturbed part of the valence band lies above the Fermi level. The density of the initial states, N_i is proportional to $E_v^{1/2}$, where E_v is the energy of the state with respect to the edge of the parabolic valence band, as shown in Figure 1.

RESULTS AND DISCUSSION

The absorption spectra of the MSe_2 (M=Nb, Mo, Ta and W) single crystals are shown in Figure 2. A careful study of these spectra revealed the presence of absorption edges in the spectral range of 700–850 nm.

To analyze the results from these spectra in the vicinity of the absorption edge based on two- and three-dimensional models, the absorption coefficient α values were determined at intervals of 5 nm. The interpretation of the experimental results, that is, the dependence of the absorption coefficient 'α' in terms of direct and indirect transitions, can be performed with the help of formulae 1 and 2 using the values of r equal to ½ and 2, respectively.

$$\alpha h\nu = A(h\nu - E_g)^r \quad (1)$$

for direct transitions and

$$\alpha h\nu = \sum_i B_i (h\nu - E_g' \pm E_p)^r \quad (2)$$

for indirect transitions.

PRINT ISSN No. 2277 - 8179 | DOI : 10.36106/ijsr

Accordingly, Figure 3 for the MSe_2 (M=Nb, Mo, Ta, and W) single crystal shows the spectral variation of $(\alpha h\nu)^{1/2}$ vs hν. Because the curves indicate discontinuous straight lines, it is possible that they represent indirect interband transitions involving the emission and absorption of phonons. To accurately determine the points of discontinuities, we followed the method successfully used for layered

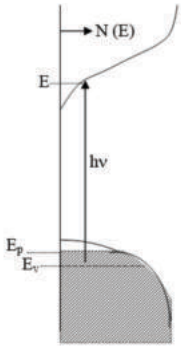

Figure 1 Energy diagram illustrating how absorption probes the conduction band tail of states in a p-type semiconductor. The tail of the valence band has been omitted since, being empty, it does not participate in the absorption process.

Accordingly, from the graphical differentiation of the data presented in figure 3 for MSe_2 (M=Nb, Mo, Ta, and W) single crystals, the dependence of the derivatives $\delta(\alpha h\nu)^{1/2}/ h\nu$ on hν is shown in Figure 4. It can be clearly seen from these figure that the derivatives are step functions of energy, with four steps well defined in the range

$$E_1 < E < E_2 , E_2 < E < E_3 ,$$
$$E_3 < E < E_4 \text{ and } E_4 < E.$$

These values of E_1, E_2, E_3 and E_4 indicate the points of discontinuity in the plots of $\delta(\alpha h\nu)^{1/2}/ \delta h\nu$ vs. hν.

The indirect energy gaps obtained from the values of E_1, E_2, E_3 and E_4 are given by:

$$E_g' = \frac{E_1 + E_4}{2} = \frac{E_2 + E_3}{2} \quad (3)$$

$$E_{p1} = \frac{E_4 - E_1}{2} \text{ and } E_{p2} = \frac{E_3 - E_2}{2} \quad (4)$$

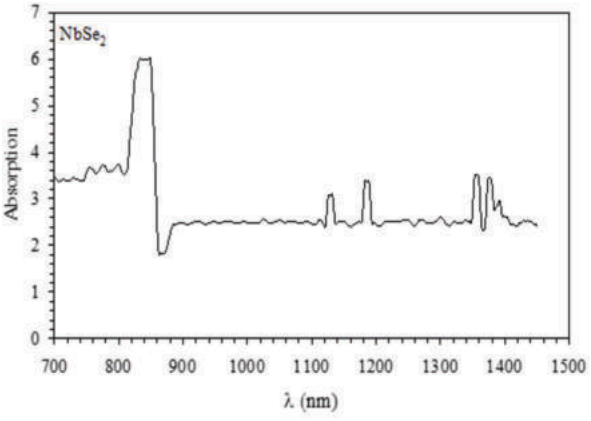

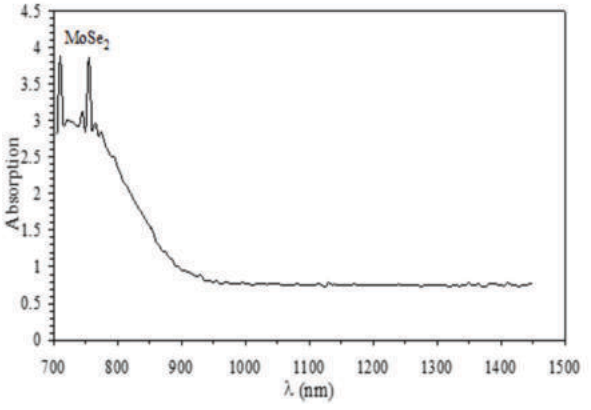

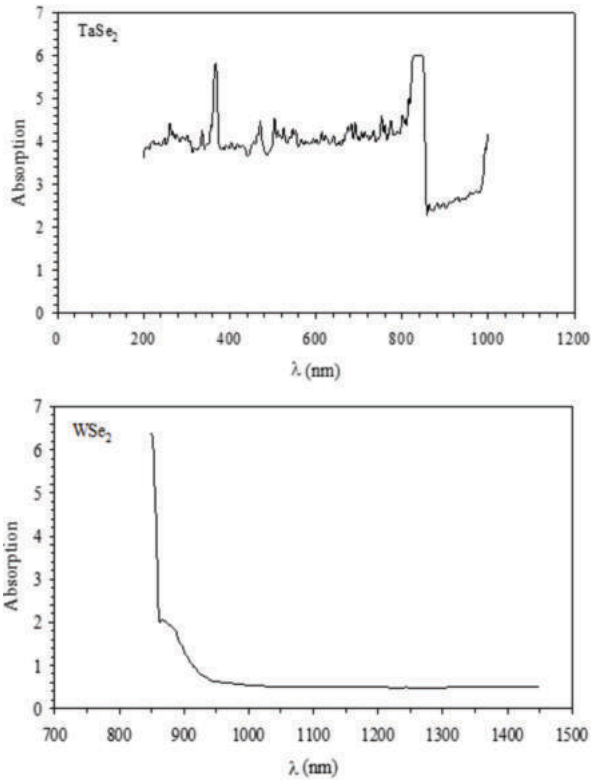

Figure 2 The Graph of Optical Spectrum for as Grown Crystals of Mse2

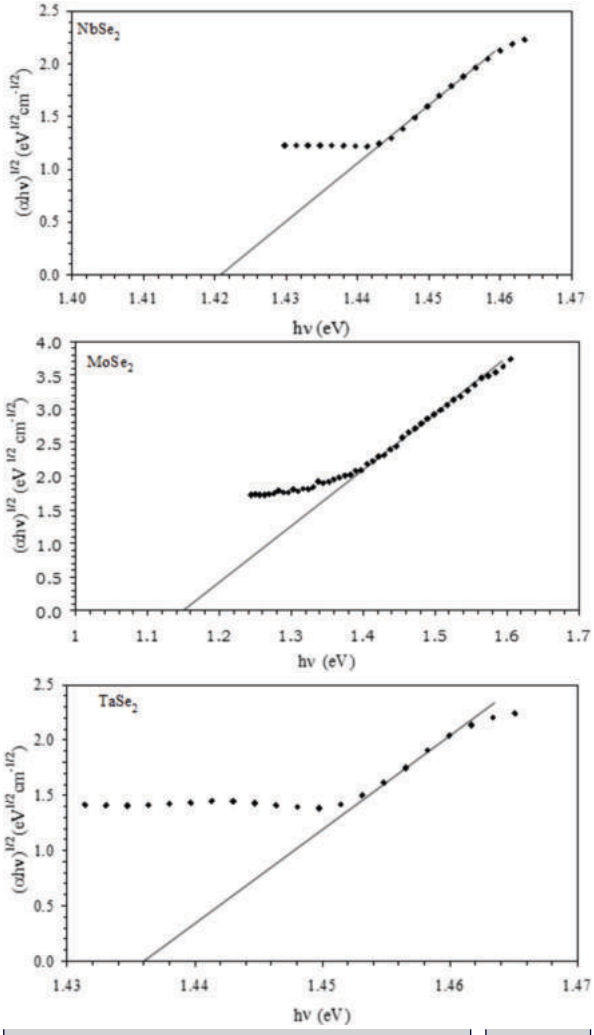

PRINT ISSN No. 2277 - 8179 | DOI : 10.36106/ijsr

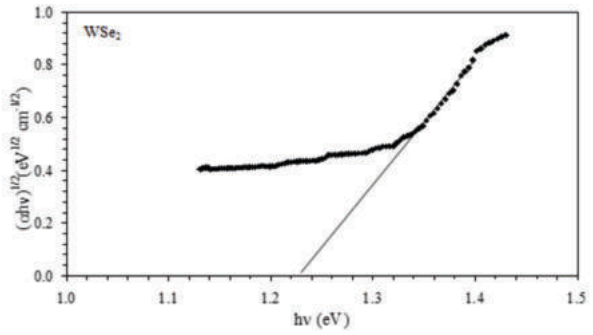

Figure 3 The Graph of (vhv)1/2 Versus hv for as Grown Crystals of MSe2

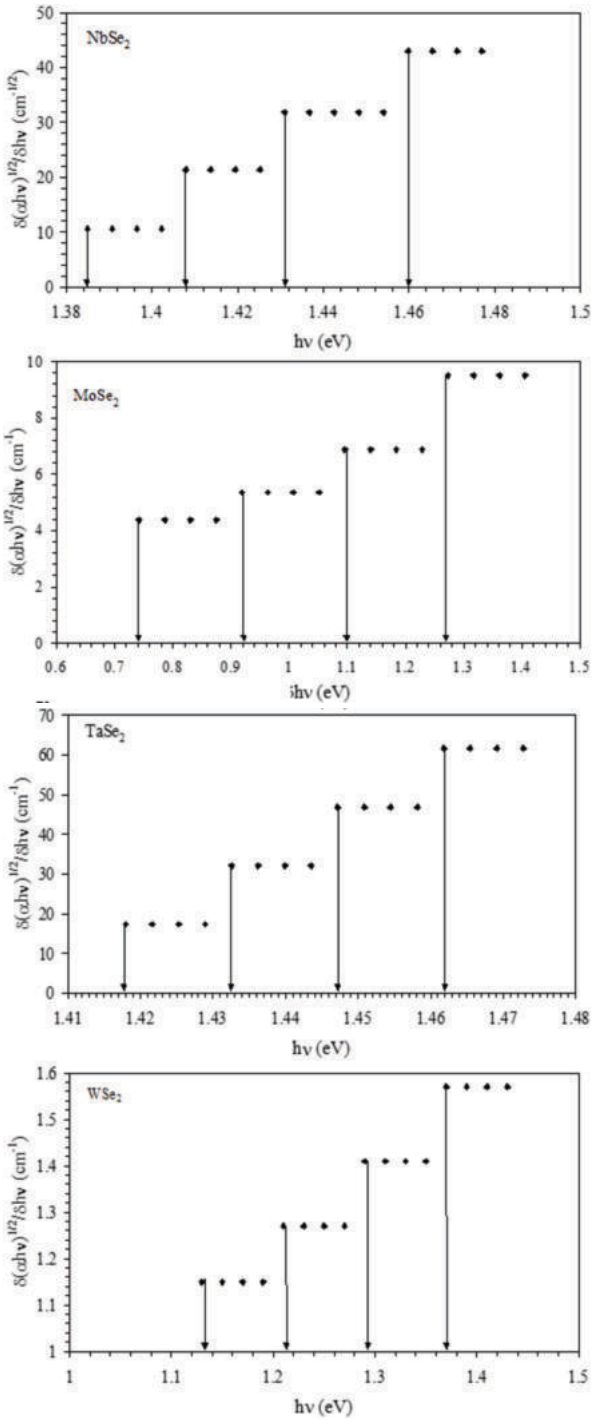

Figure 4 The Spectral Variation of δ(δhv)1/2/δhv Versus hv for as Grown Crystals of MSe2

The values of the indirect band gap E'_g and phonon energies thus obtained are presented in Table 1. The values of gE′ can also be obtained from the intersection of the linear portion of the curves with the energy axis for zero absorption, as shown in figure 3. These values closely match the values obtained from formula 3.

To determine the direct band gap E_g, the spectral variation of $(hv)^2$ vs. hv, as shown in Figures 5 were studied. The values of direct band gap E_g obtained from the intersection of the linear portion of the curves in figure 5 are listed in Table 1.

Table 1 Optical Parameters for as Grown Crystals of MSe_2 (M = Nb, Mo, Ta and W)

Parameters	NbSe2	MoSe2	TaSe2	WSe2
E1 (eV)	1.38	0.74	1.42	1.13
E2 (eV)	1.41	0.92	1.43	1.21
E3 (eV)	1.43	1.10	1.45	1.29
E4 (eV)	1.46	1.27	1.46	1.37
Ep1 (eV)	0.04	0.27	0.02	0.12
Ep2 (eV)	0.01	0.09	0.01	0.04
1 (K)	464	3134	232	1393
2 (K)	116	1044	116	464
Eg (eV)(Direct)	1.44	1.40	1.45	1.41
(C)(eV)	1.42	1.00	1.44	1.23
(E) (eV)	1.42	1.14	1.43	1.23
Band tailing E0	0.03	0.04	0.03	0.03
Actual band gap (-E0) (eV)	1.39	1.10	1.40	1.20

'gE(C) = Indirect band gap from the calculation
(E) = indirect band gap from extrapolation

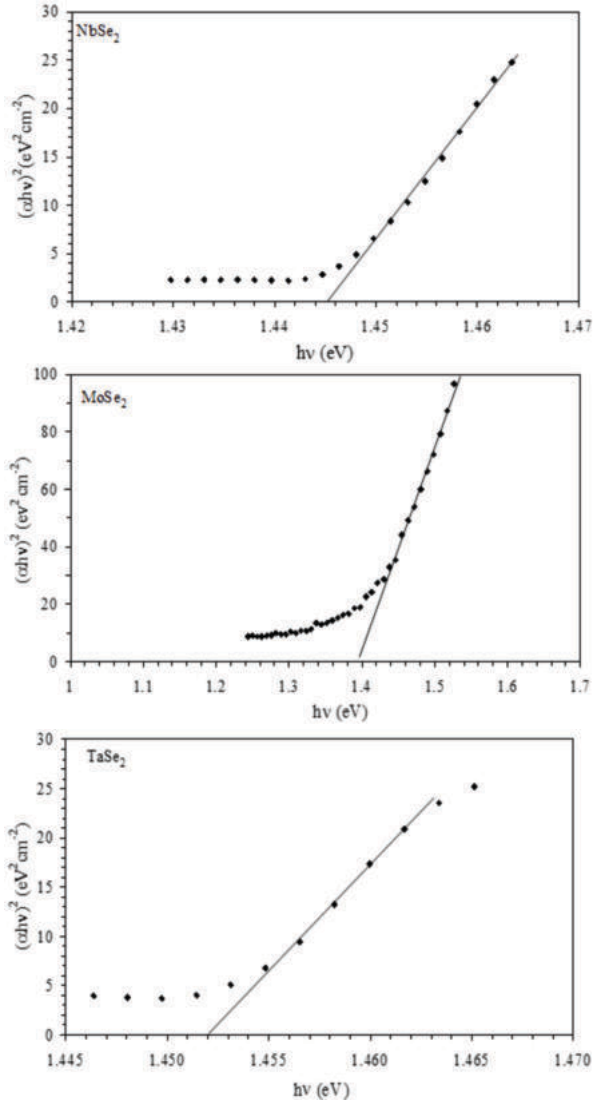

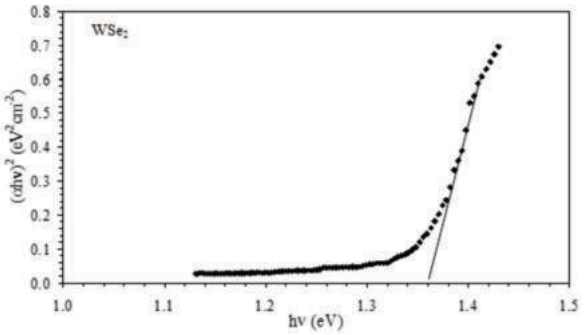

Figure 5 The Graph of (αhν)2 Versus hν for as Grown Crystals of MSe2

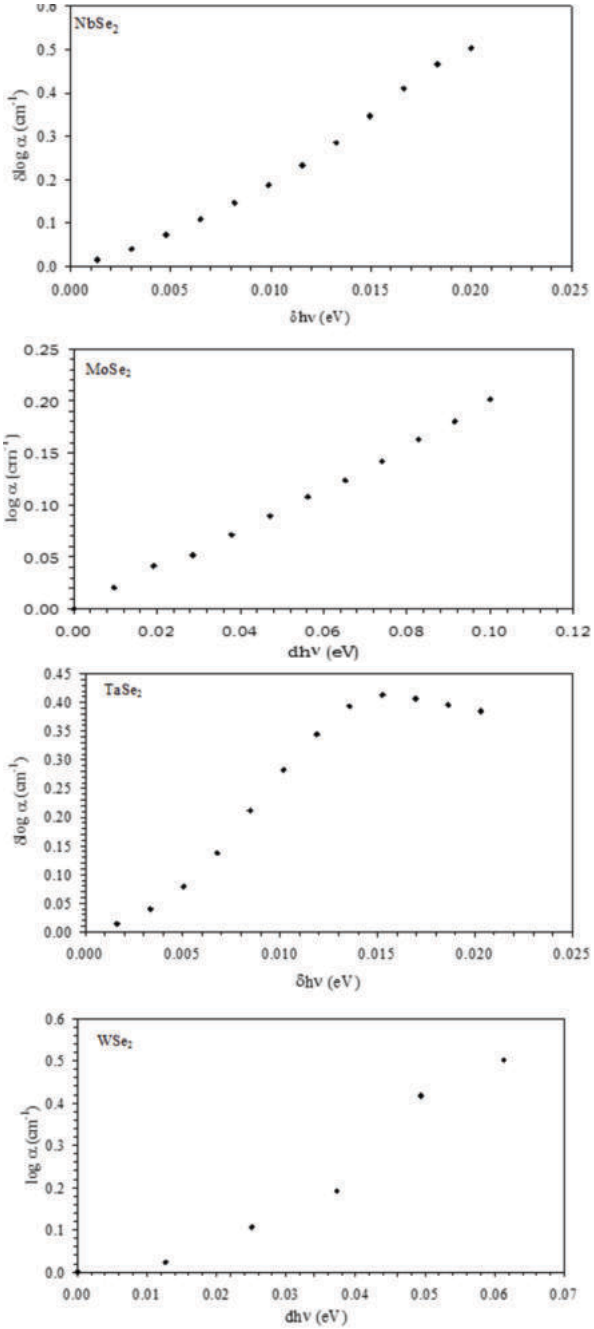

Figure 6 The Graph of Log α Versus αhν for as Grown Crystals of MSe2

CONCLUSION

- The optical parameters of MSe_2 (M = Nb, Mo, Ta, W) single crystals strongly depend on the transition- metal species.
- The critical point energies (E_1–E_4) increase systematically from $MoSe_2$ to $TaSe_2$ and $NbSe_2$ due to variations in d-orbital hybridization and spin–orbit coupling.
- $MoSe_2$ exhibited lower transition energies, indicating a relatively narrower electronic band structure.
- $TaSe_2$ and $NbSe_2$ exhibit higher transition energies, reflecting stronger metal–chalcogen bonding.
- Plasmon energies (E_{p1}, E_{p2}) are smaller for $NbSe_2$ and $TaSe_2$, while $MoSe_2$ and WSe_2 show enhanced plasmon contributions.
- The higher plasmon energies suggest increased free-carrier participation and dielectric response in $MoSe_2$ and Wse_2.
- The large oscillator strengths of $MoSe_2$ indicate stronger optical transitions and higher polarizability.
- All compounds exhibit direct band gaps in the range of 1.40–1.45 eV, which are suitable for optoelectronic applications.
- Band tailing effects reduce the actual band gaps, particularly in $MoSe_2$ and WSe_2, owing to localized states.
- Overall, metal selection effectively tunes the optical properties of MSe_2, making it promising for photonic and optoelectronic devices.

REFERENCES

[1] M. Munkhbat, P. Wróbel, T. J. Antosiewicz, T. Shegai, and A. V. Zayats, "Optical constants of several multilayer transition metal dichalcogenides measured by spectroscopic ellipsometry in the 300–1700 nm range: High index, anisotropy, and hyperbolicity," ACS Photonics, vol. 9, no. 8, pp. 2398–2407, 2022.
[2] Y. Wang and X. Zhang, "Experimental and theoretical investigations of direct and indirect band gaps of Wse_2," Micromachines, vol. 15, no. 6, p. 761, 2024.
[3] T. N. Do, P. H. Shih, and G. Gumbs, "Optical absorption of TaS_2 and $TaSe_2$ transition-metal dichalcogenides," Solid State Phenomena, vol. 356, pp. 113–118, 2024.
[4] B. Gul, M. S. Khan, I. Ahmad, and X. Han, "A first-principles study of the electronic, optical and transport properties of transition metal dichalcogenides," Materials Advances, vol. 4, pp. 4204–4215, 2023.
[5] J. Liu, Y. Jin, B. Lei, X. Zhao, Y. Huang, L. Zhang, and Y. Zhu, "Electronic structure and optical properties of MoS_2-based heterojunctions with transition metal dichalcogenides," Catalysts, vol. 14, no. 10, p. 678, 2024.
[6] V. Rodionov, A. Ivanov, M. Glazov, and D. Efimkin, "Excited states of excitons in $MoSe_2$ and WSe_2 monolayers," JETP Letters, vol. 120, pp. 270–276, 2024.
[7] A. Kormányos et al., "k·p theory for two-dimensional transition metal dichalcogenide semiconductors," 2D Materials, vol. 2, no. 2, p. 022001, 2015.
[8] K. L. Chopra and L. L. Miller, "Optical absorption in layered transition-metal dichalcogenides," Physical Review, vol. 176, no. 1, pp. 184–193, 1968.
[9] W. Baltensperger, "On the theory of impurity absorption in semiconductors," Philosophical Magazine, vol. 44, no. 356, pp. 1355–1368, 1953.
[10] P. Aigrain, "Optical properties of semiconductors with impurities," Physica, vol. 20, no. 1–6, pp. 978–990, 1954.
[11] R. H. Parmenter, "The optical absorption edge in heavily doped semiconductors," Physical Review, vol. 97, no. 3, pp. 587–598, 1955.
[12] E. O. Kane, "Band structure of indium antimonide," Physical Review, vol. 131, no. 1, pp. 79–88, 1963.
[13] B. I. Halperin and M. Lax, "Impurity-band tails in the high-density limit," Physical Review, vol. 148, no. 2, pp. 722–740, 1966.
[14] T. S. Moss, "The interpretation of the properties of indium antimonide," Journal of Applied Physics, vol. 32, no. 10, pp. 2136–2139, 1961.
[15] D. E. Hill, "Phonon-assisted optical absorption in semiconductors," Physical Review, vol. 133, no. 3A, pp. A866–A874, 1964.
[16] J. I. Pankove, "Optical processes involving phonons in semiconductors," Physical Review, vol. 140, no. 6A, pp. A2059–A2065, 1965.
[17] F. Urbach, "The long-wavelength edge of photographic sensitivity and of the electronic absorption of solids," Physical Review, vol. 92, no. 5, pp. 1324–1324, 1953.
[18] K. K. Kam, C. L. Chang, and D. W. Lynch, "Optical properties of metallic and semiconducting transition metal dichalcogenides," Journal of Physics C: Solid State Physics, vol. 17, no. 23, pp. 4031–4040, 1984.
[19] V. M. Koshkin, V. R. Karas', and P. S. Gal'chinetskii, "Optical absorption edge and impurity states in layered semiconductors," Soviet Physics–Semiconductors, vol. 3, no. 10, pp. 1186–1189, 1970.
[20] D. A. Dholakiya, G. K. Solanki, S. G. Patel, and M. K. Agarwal, "Optical absorption and band gap studies in layered semiconducting crystals," Bulletin of Materials Science, vol. 24, no. 3, pp. 291–296, 2001.
[21] D. A. Dholakiya, G. K. Solanki, S. G. Patel, and M. K. Agarwal, "Optical properties and band tailing effects in layered semiconductors," Scientia Iranica, vol. 10, no. 4, pp. 373–378, 2003.